Detection of unstable periodic orbits in mineralising geological systems

S. Oberst, R. K. Niven, D. R. Lester, A. Ord, B. Hobbs, and N. Hoffmann

Citation: Chaos **28**, 085711 (2018); doi: 10.1063/1.5024134
View online: https://doi.org/10.1063/1.5024134
View Table of Contents: http://aip.scitation.org/toc/cha/28/8
Published by the American Institute of Physics

Detection of unstable periodic orbits in mineralising geological systems

S. Oberst,[1,a)] R. K. Niven,[2] D. R. Lester,[3] A. Ord,[4] B. Hobbs,[5] and N. Hoffmann[6]
[1]*Centre for Audio, Acoustics and Vibration, University of Technology Sydney, Broadway, Sydney, New South Wales 2007, Australia*
[2]*School of Engineering and Information Technology, The University of New South Wales, Canberra, Northcott Drive, Campbell, Australian Capital Territory 2600, Australia*
[3]*School of Engineering, Royal Melbourne Institute of Technology, GPO Box 2476, Melbourne, Victoria 3001, Australia*
[4]*Centre for Exploration Targeting, The University of Western Australia, 35 Stirling Highway Crawley, Perth, Western Australia 6009, Australia*
[5]*Commonwealth Scientific and Industrial Research Organisation, 26 Dick Perry Ave., Kensington, Western Australia 6152, Australia*
[6]*Dynamics Group, Complex Systems, Mechanical Engineering, Technical University Hamburg, Schlossmühlendamm 30, 21073 Hamburg, Germany*

(Received 30 January 2018; accepted 24 July 2018; published online 24 August 2018)

Worldwide, mineral exploration is suffering from rising capital costs, due to the depletion of readily recoverable reserves and the need to discover and assess more inaccessible or geologically complex deposits. For gold exploration, this problem is particularly acute. We propose an innovative approach to mineral exploration and orebody characterisation, based on the analysis of geological core data as a spatial dynamical system, using the mathematical tools of dynamical system analysis. This approach is highly relevant for orogenic gold deposits, which—in contrast to systems formed at chemical equilibrium—exhibit many features of nonlinear dynamical systems, including episodic fluctuations on various length and time scales. Feedback relationships between thermo-chemical and deformation processes produce recurrent fluid temperatures and pressures and the deposition of vein-filling minerals such as pyrite and gold. We therefore relax the typical assumption of chemical equilibrium and analyse the underlying processes as aseismic, non-adiabatic, and inherent to a hydrothermal, nonlinear dynamical open-flow chemical reactor. These processes are approximated using the Gray-Scott model of reaction-diffusion as a complex toy system, which captures some of the features of the underlying mineralisation processes, including the spatiotemporal Turing patterns of unsteady chemical reactions. By use of this analysis, we demonstrate the capability of recurrence plots, recurrence power spectra, and recurrence time probabilities to detect underlying unstable periodic orbits as one sign of deterministic dynamics and their robustness for the analysis of data contaminated by noise. Recurrence plot based quantification is then applied to three mineral concentrations in the core data from the Sunrise Dam gold deposit in the Yilgarn region of Western Australia. Using a moving window, we reveal the episodic recurring low-dimensional dynamic structures and the period doubling route to instability with depth, embedded in and originating from higher-dimensional processes of the complex mineralisation system. *Published by AIP Publishing.* https://doi.org/10.1063/1.5024134

The exploration of ore deposits is challenging owing to increased costs and a decreasing abundance of commodities. The precipitation of minerals occurs over a long time span, and chemicals and mineral solutions are exposed to temperature and pressure gradients with dynamics possibly far away from equilibrium; the underlying dynamical processes are yet unknown, and whether low dimensional deterministic dynamical features can be evidenced is an open question. By applying nonlinear time series analysis tools, in particular, recurrence plots and associated recurrence power spectra to drill core data—analysed as a spatial series—from the Yilgarn region in Western Australia, we show for the first time the presence of recurrent deterministic structures. The investigated recurrent states mark the presence of stable or unstable periodic orbits, a unique sign of low dimensional, nonlinear deterministic dynamics embedded in a high dimensional system.

I. INTRODUCTION

According to the Minerals Council Australia, 44% of today's mining projects explore new prospective gold deposits—a consequence of a significantly risen gold price, high demand on the market, and a decreasing average yield in the mines.[1] However, considering the decreasing profitability in the mining industry, the process of exploring economically a large gold deposit is significant with respect to time and facilities involved. New gold deposits are nowadays more difficult to delineate from economically less important mineral deposits; in addition, the ore quality, that is, the deposited gold, is of increasingly lower grade with depth, which is

a)Also at Dynamics Group, Complex Systems, Mechanical Engineering, Technical University Hamburg, Schlossmühlendamm 30, 21073 Hamburg, Germany and School of Engineering and Information Technology, The University of New South Wales, Canberra, Northcott Drive, Campbell, ACT 2600, Australia. Electronic mail: sebastian.oberst@uts.edu.au. URL: http://www.uts.edu.au/staff/sebastian.oberst.

problematic for the Australian mining sector.[2] Innovative exploration and analysis approaches to study test core data are therefore sought.[3]

Mineralogy content of deposit samples is traditionally measured using, for example, optical metrology using spectral imaging techniques (via refractive index and dispersion), complemented by digestive chemical analyses.[4,5] Using statistical techniques and assuming chemical equilibria, changes are generally attributed to external system processes of seismic events, adiabatic fault-valve, or suction pump/piston behaviour.[6] However, the precipitation of minerals and gold follows chemical exo- and endothermic autocatalytic processes, which are generally interpreted as thermodynamic non-equilibrium processes exhibiting episodic oscillations—inherent characteristics of nonlinear dynamical systems.[4,7,8] Non-equilibrium systems are manifold and often encountered in physics, e.g., the Rayleigh–Bénard convection. Opposed to stochastic dynamic systems, such as those which may be modelled using the Fokker-Planck equation, the non-equilibrium systems studied here remain bounded and generate new information but without necessarily changing their probability distribution.[7,9,10] Alternatively, such oscillations could be considered to arise in a random dynamical system, undergoing either a Hopf bifurcation or stochastic induced auto-oscillations.[11,12] Feedback relations between thermo-chemical deformation processes lead to oscillatory behaviours in temperature, chemical potential, or fluid pressures and the deposition of vein filling materials, pyrite, and gold over multiple time and spatial scales.[13–15] Chemical reactions related to mineralising systems have been modelled as Lynch's continuously stirred chemical reactor[16] or as reaction-diffusion equations similar to the Gray-Scott model (GSM),[4,17,18] the latter originating from a simplification of the autocatalytic processes underlying the Selkov model of glycolysis reactions.[19] Both benchmark systems exhibit a variety of reaction patterns of chemical species characteristic of autocatalytic processes including periodic, quasi-periodic, and chaotic dynamics, travelling waves or Turing patterns—including various time—and also length-scales.[16,20,21] We assume that processes leading to mineralisation and gold precipitation are aseismic, non-adiabatic, and confined to the mineralising system, which behaves like a spatially distributed network of hydrothermal, open-flow chemical reactors.[16,20,21]

Nonlinear dynamic features and deterministic chaos[9] are common in information-generating (positive entropy, non-equilibrium) natural processes and therefore also often evidenced in technical applications;[22–25] however, the onset of unstable periodic orbits also marks the loss of the system's long-term predictability and hence problems in the ability to reliably control its dynamics. Spatiotemporal chaos has been rarely studied in connection with recurrence plot quantification, and it is less studied compared to temporal chaos.[7,9,26]

Hydrothermal systems show typical characteristics of spatially extended nonlinear dynamical systems in non-equilibrium states:[4,5] (1) large gradients of concentrations of chemical species, (2) mineralogy with spatial patterning within rocks and the hydrothermal alteration envelope[27] or beyond the ore body; (3) stronger mineralisation around large gradients of hydrogen ions (pH) and electron activity (Eh), possibly spatially fractal and apparent irregular;[5] (4) a mineralising phase combined with fracturing, veining, stockwork formation, or brecciation (e.g., Witwatersrand system[5]); (5) time-relatedness in the form of paragenetic sequence (spatial over-printing); and (6) a strong dependence on initial conditions.

To answer questions of how measured data are related to nonlinear dynamics involved, recurrence plots[28] have emerged as a popular tool in nonlinear science in the recent years and have been applied in different variations to problems in ecology,[29] in chemistry, physics, and medicine,[30–32] to economic questions,[33] to engineering problems,[34,35] or to seismological questions.[36] Recurrence plots have been used in the past (1) to visualise/qualify *unstable* periodic orbits of a chaotic attractor by simultaneously (2) studying its system dynamics.[8,9,37] Application to mineralising systems might allow identifying hidden patterns also in geology. Specifically, the question whether patterning in spatially-extended geological systems can be classified or associated with deterministic dynamics as *vectors towards mineralisation* remains to be answered.[5] Since mineralisation systems are very complex, and high dimensional, we especially raise the question whether these systems respond in certain conditions with dominating low dimensional processes at certain scales; in this context, weak high-dimensional dynamics are interpreted as noise.

Here, we study the GSM as a uni-directionally coupled, flow-driven chemical system and—without explicitly modelling mineralisation processes—we assume their relatedness to test for similarities in model responses.[21] We study the capability of the GSM of exhibiting non-stationary spatiotemporal episodic fluctuations,[38] and by being coupled to multiplicative noise, we study the potential of detecting unstable periodic orbits using nonlinear filtering and recurrence plots. Multiplicative noise represents here the higher dimensional processes interwoven with the mineralising system. The Hénon map as an additional benchmark of a time-discrete system (contaminated with *additive* noise, inherent to every measuring process as observational or channel noise) is provided in the supplementary material. Finally, we apply nonlinear filtering and recurrence plot quantification to study the existence of deterministic nonlinear dynamic features, namely, unstable periodic orbits on real-life experimental drill-core data of mineral abundance.[8,39,40] While the results of the GSM and the Hénon map simply establish the methodology, an existence of unstable periodic orbits in mineralising systems would contradict the widespread assumption that a geological system is in a chemical equilibrium.

II. METHODS, MODELS, AND EXPERIMENTS

A. Gray-Scott model of reaction-diffusion

The emergence of spatial structures and irregular distribution patterns in mineral deposits is caused by the interplay of several chemical and physical processes across a multitude of chemical, including fluid transport, exo- and endo-thermic chemical reactions, precipitation, and dissolution. Chemical species being solved in a fluid are constrained by porous rocks

which are influenced by temperature, high pressure gradients, and mechanical loads (e.g., brecciation).[5]

Reaction and diffusion in chemical species represent fundamental mechanisms for fractal pattern in mineral deposits.[7,41,42] While Lynch's model of coupled exothermal reactions[6,16] also includes advection, it does not include spatial characteristics and diffusivity which can be modelled using the relatively simple Gray-Scott model (GSM) of reaction-diffusion.[20] Coupled reaction-diffusion systems, such as hydrothermal metasomatic rock formations, can induce unstable, spontaneous dynamics.[43] Similar behaviour is shown by the GSM which also exhibits sub- and supercritical Hopf as well as Turing bifurcations.[20] The GSM simulates a cubic autocatalytic chemical reaction including the decay of reactants U (inhibitor) and V (activator, catalyst) to a product P, represented using binary chemical reactions[7] $U + 2V \rightarrow 3V$ and $V \rightarrow P$. The GSM exhibits both sub- and supercritical Hopf as well as Turing bifurcations[20] and can mathematically be expressed via

$$\frac{\partial u}{\partial t} = r_u \nabla u - uv^2 + f(1-u), \tag{1}$$

$$\frac{\partial v}{\partial t} = r_v \nabla v - uv^2 - (f-k)v, \tag{2}$$

with $u := u(x, y, t)$ and $v := v(x, y, t)$ representing time-dependent and spatially varying (x being the one for *depth*), but dimensionless concentrations (mole fractions) of the inhibitor and the catalyst, respectively, with r_u and r_v being their diffusivities; f represents the process rate (that feeds V and drains U), and k is the conversion rate to product P.

Real life experimental data of mineral drill core data are spatially extended data and only accounts for one time slice involved, removing time dependency in principle owing to the large time scales involved: Crustal developments reach usually back many millions if not billions of years.[44] Hence, for the analysis of the GSM, we simulated the development of $u(x, y, t)$ and used a spatial domain of 80 times 4660 pixels to generate a swirling, oscillatory pattern:[45] we set $k = 0.053$ and $f = 0.0261$ (hence $f - k > 0$) and used the diffusivities $r_u = 1$ and $r_v = 0.524$. To validate whether the GSM has reached a steady-state and to keep the computational burden low, 20 randomly drawn points within the GSM domain were monitored for 100 000 s simulation time; after about 40 000 s most of the initial transients have died out but only in the centre and after about 90 000 s a *quasi steady-state* was reached (supplementary material, Fig. S1). We extracted a scalar spatial vector $\mathbf{u}(x) = \mathbf{u}(x, y = const., t = const.)$ at the centre of the simulation domain with a length of 4660 samples (assuming 10 pixels correspond to 1 m). To generate an observer function $\tilde{\mathbf{u}}$ as a surrogate of real-life data drill core data, the vector was multiplied with uniformly distributed, and $ns = 0.1$-weighted white noise $\mathbf{wn}$. We use the spatial domain to simulate simple chemical processes in space; hence, it is not expected that the GSM is able to simulate the complex geological mineral precipitation processes; it solely serves the purpose of demonstrating the performance of the nonlinear filtering of multiplicative noise as well as showing the capability of the recurrence power spectrum to detect unstable periodic orbits in the presence of noise:

$$\tilde{\mathbf{u}}(x) = \mathbf{u}(x) + ns \cdot \mathbf{wn} \circ \mathbf{u}(x). \tag{3}$$

This *static* model does not effect the dynamics directly as it considers that the (observational) noise after the oscillatory data has been extracted. However, its absolute value depends on the magnitude of oscillation, providing a multiplicative, that is, nonlinear coupling.[46] Multiplicative noise is generally more challenging to be removed compared to simple additive (channel or observational) noise.[8,47] Both additive and multiplicative noise are considered here as they represent either observational noise or possibly high-dimensional contributions to the dynamics—and both could be interfering with the quantification based on recurrence plots.

B. Experimental data

The experimental data originate from drill-hole infrared reflectance measurements from the Sunrise Dam gold mines in the Yilgarn region of Western Australia, formed in the Neoarchean (ca. 2700–2400 Ma).[48] We have already shown that drill-hole data and chemical compositional data indicate recurrent states.[15] However, our previous research data[15] had only averaged mineralogical and chemical data of a rather coarse sampling rate with a depth of 1 m.[14] Here, the abundance of amphibole, carbonate, and sericite was measured using hyper-spectral imaging techniques. Amphibole is an inosilicate mineral often present in green schist grade alteration associated with lode-gold deposits.[44] Carbonate enrichment is related to hydrothermal alteration as both vein-filling and host rock alteration; sericite is a hydrothermal alteration product of feldspars; both these mineral assemblages may be part of the same mineral reaction system and are commonly intimately associated with high gold concentrations.[49] Only integer concentrations were recorded which had many zero-valued entries, but recording was conducted using a fine 1.65 mm spatial resolution over a sample depth of about 466 m.

The log abundance of mineral data for the mineral assemblages of amphibole, carbonate, and sericite complexes is depicted in Figs. 1(a)–1(c). To overcome the coarse resolution in the abundance measurements, the data were transformed by taking the log of the interval depths between measurements of non-zero abundance so that fluctuations indicated the non-existence of the measured mineral [Figs. 1(d)–1(f)]. It is expected that the transformation produces the same statistical distribution for all three minerals and reduces thereby the amount of data and making it more comparable.[46] Using distances between non-zero events is similar to measuring the laminar time spans when analysing the intermittency routes to chaos or measuring the time between droplets of a dripping faucet; the dynamics are reduced to those of a map whose temporal connectedness is preserved.[9,25] Map data are computationally less heavy; therefore, reducing the data to a discrete set of points also alleviates the *curse of dimensionality*.[50]

III. METHODS USED

Coming from real-life drill core measurements of spectral data of mineral abundance, it is our purpose to generate a topological invariant set, a so-called attracting set out

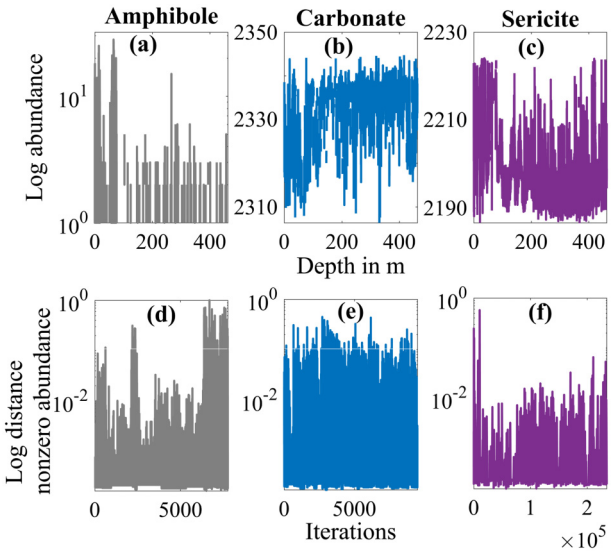

FIG. 1. [(a)–(c)] Abundance of amphibole, carbonate, and sericite against bore hole depth and [(d) and (e)] distance between events of nonzero abundance against number of iterations.

of our dynamics.[51] For this reconstruction, the dynamics is required to be embedded in phase space using embedding theorems.[52] This reconstructed attracting set is then used to calculate recurrence matrices and to estimate recurrence quantification measures. Here, we use delay embedding, for which we require a suitable delay and an appropriate embedding dimension. To estimate an appropriate shift (delay), the first minimum of the averaged auto-mutual information is chosen,[47,53,54]

$$I(\tilde{U};\tilde{U}_\tau) = \sum_{\tilde{u}\in\tilde{U}}\sum_{\tilde{u}_\tau\in\tilde{U}_\tau} p(\tilde{u},\tilde{u}_\tau)\log_2\left(\frac{p(\tilde{u},\tilde{u}_\tau)}{p(\tilde{u})p(\tilde{u}_\tau)}\right), \quad (4)$$

with $\tilde{u}(x+\tau)=u_\tau$ describing a component of the observation vector [Eq. (3)] shifted in space by the parameter τ[53] and $\tilde{U}$ representing the whole set of observations $\tilde{\mathbf{u}}$. The numerator and denominator in Eq. (4) represent the joint and the marginal density functions. Taking the first minimum of $I(\tilde{U};\tilde{U}_\tau)$ provides a delay at which by τ shifted embedding space vectors are minimally correlated.[55] Then, the false nearest neighbour algorithm[47,53,54] can be used to embed the (space-) shifted observable $\tilde{\mathbf{u}}(y+\tau)$ in a phase space of increasing dimensions; once a minimum of false nearest neighbours is reached, the attractor can be regenerated. The smallest dimension with a minimum of false nearest neighbours (generally less than 10% of false neighbours) marks the minimum embedding dimension m required to house the dynamics within a vector subspace $\mathcal{S}$ formed by the delay vectors as place holder of the original invariant set,[52,53,56]

$$\mathcal{S} = \langle\tilde{u}(x),\tilde{u}(x+\tau),\ldots\tilde{u}[x+(m-1)\tau]\rangle. \quad (5)$$

Once the dynamics is reconstructed, a recurrence plot can be generated. A recurrence plot (RP) is a graphical representation of the recurrence matrix, which compares the pairwise distances of phase space vectors and visualises information regarding spatial correlations across multiple scales. A RP is suitable for stationary and non-stationary data, and short time signals show a high robustness against noise. Similar to a short-time Fourier transform, a RP indicates also where dominant frequencies occur,[37,51,54]

$$R_{i,j} = \Theta(\epsilon - ||\tilde{u}_i - \tilde{u}_j||_2) \in \{0,1\} \quad \text{for } i,j = 1\ldots N, \quad (6)$$

with $R_{i,j}$ being one entry in the recurrence matrix with Θ being the Heavyside function, $\tilde{u}(i)=u_i$ being a component of the delay-embedded phase space vector, and $\tilde{u}_j=\tilde{u}(j)=\tilde{u}(i+\tau)$ being a τ-delayed vector component; and i as related to x_i being the point in space associated with the i-th observation (cf. Ref. 57). $||\cdot||_2$ represents the L_2 norm[54] calculating the Euclidean distance between two points in phase space; the ϵ represents the threshold criterion which is set, according to the *fixed amount of neighbours* (FAN) criterion, to always contain the same percentage of neighbours (fixed recurrence point density) relative to all dynamic states resulting in an asymmetric recurrence matrix.[28] The FAN neighbourhood criterion is adaptive to the dynamics by resolving scaling issues and handling non-stationarity better than a fixed neighbourhood criterion[54,58]

From line structures formed in a RP, histograms and quantification measures can be estimated; diagonal lines depicted within a RP correspond to recurrent dynamical states, whereas vertical/horizontal lines (and blocks) indicate trapped dynamics as, e.g., found for zero values.[54] Here, we use the recurrence rate (RR) which is defined as the density of recurrent states in a recurrence plot and which is proportional to the probability that a certain dynamic state repeats itself. The mean recurrence time (RT) represents the average time between recurrent events; RR and RT are defined as follows:

$$\text{(a) RR} = \frac{1}{N^2}\sum_{i,j}^{N} R_{i,j} \quad \text{and} \quad \text{(b) RT} = \frac{\sum_{v=1}^{N} vp(v)}{\sum_{v=1}^{N} p(v)}. \quad (7)$$

Here, N is the length of the trajectory and $p(v)$ is the mean of the frequency distribution of white vertical lines of length v.[59] Zbilut and Marwan[40] applied the Wiener-Khinchin theorem to the recurrence rate and showed that its power spectral density constitutes a generalisation of the power spectra calculated with the auto-covariance function but without having the limitation of being only applicable to linear, stationary data. Here, we use Welch's power spectral density estimate (*modified* Barlett method[60]) and compare it to recurrence rate-based power spectra (cf. Refs. 8 and 40). Welch's spectrum reduces noise with the trade-off of also decreasing the frequency resolution.[60] A window of length of 2^9 samples (and 2^8 FFT lines) was chosen with 50% overlap.

To generate the RT, the observation vector is divided into shorter segments of length L for which each RT is calculated. Here, $L=N$ is chosen[8] and the recurrence probability is estimated over the histogram of recurrence times against the sampling frequency two times the maximum recurrence time. To nonlinearly filter the data, the *ghkss* algorithm of the TISEAN package[56] is applied, which is based on separating low and high dimensional dynamics by projecting the dynamics on a low dimensional manifold and subtracting the noise under consideration of an assumed attractor's curvature.[8,56,61]

In this study, for all recurrence plot based calculations, we used the fixed amount of neighbour criterion and an ϵ neighbourhood, which took values of 1.5% of the maximum

phase space diameter D. The absolute maximum phase space diameter took values of $D = 1.7982$ (noise) and $D = 1.6638$ (no noise) for the synthetic GSM data, and $D = 3.73$, 4.37, and 2.31 for amphibole, carbonate, and sericite, respectively. Increasing the ϵ-neighbourhood would lead to more points in the calculations until the whole data set (attractor) is included; this, however, could lead to artefacts and the inclusion of tangential motion.[54,57] In the recurrence plot, this would result in an increasing number of solid black squares. Here, not much difference could be observed using 1.5% D compared to using 5% D; for 7% D, the spectra for sericite changed slightly, however, for 10% D, no bifurcations showed up anymore and all spectra looked rather flat but with low frequency noise (see supplementary material, Fig. S8). Decreasing the size of ϵ to below 1.5% would lead to a decrease in visibility of lines in the recurrence plot and would consequently thin out the points captured which led to a slight change the spectrum of carbonate.

IV. RESULTS AND DISCUSSION

A. Gray-Scott model of reaction-diffusion

Figure 2(a) exemplifies the results of the GSM in U using 512 samples after 90 000 s simulation time [cf. dashed vertical line Fig. 2(a)]. After a parameter study, an average delay of about $\tau = 7$ and an average embedding dimension of $m = 5$ are used for both the GSM with and without noise. As shown in Fig. 2(b), noise deteriorates the time series in particular for larger absolute values due to the multiplicative character (scaling with amplitude). Especially for the phase space, as presented in Fig. 2(c), noise becomes detrimental to the geometry of the attracting set. Similar to the GSM shown in Fig. 2, disrupted and non-stationary episodic oscillations may also be discovered in rock and mineral assemblages.[5,44,62] In case nonlinear and low dimensional dynamics exist, the reliable removal of higher dimensional processes (noise) might be a key criterion in discovering dynamic invariant sets and fractality in geological drill-hole data.

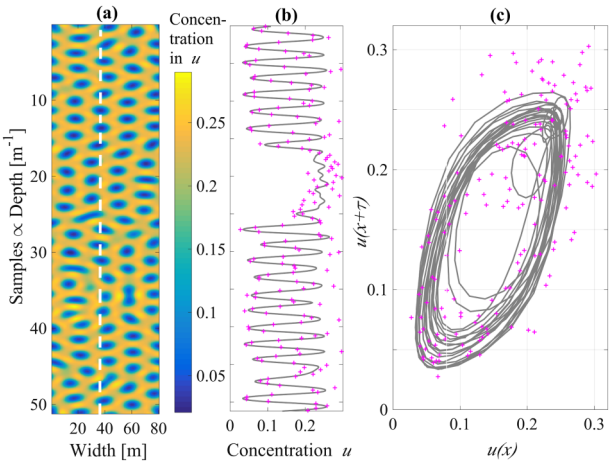

FIG. 2. Gray-Scott model of reaction-diffusion (a) after 90 000 s simulation time, dashed white line indicates the location where the sample time series has been taken from to generate the observation function $\tilde{\mathbf{u}}$, Eq. (3), (b) plot of u against depth x, extracted data $\mathbf{u}$ (solid line), and observable $\tilde{\mathbf{u}}$ (marker), and (c) phase space representation of the dynamics depicted in (b); see the supplementary material for more detail.

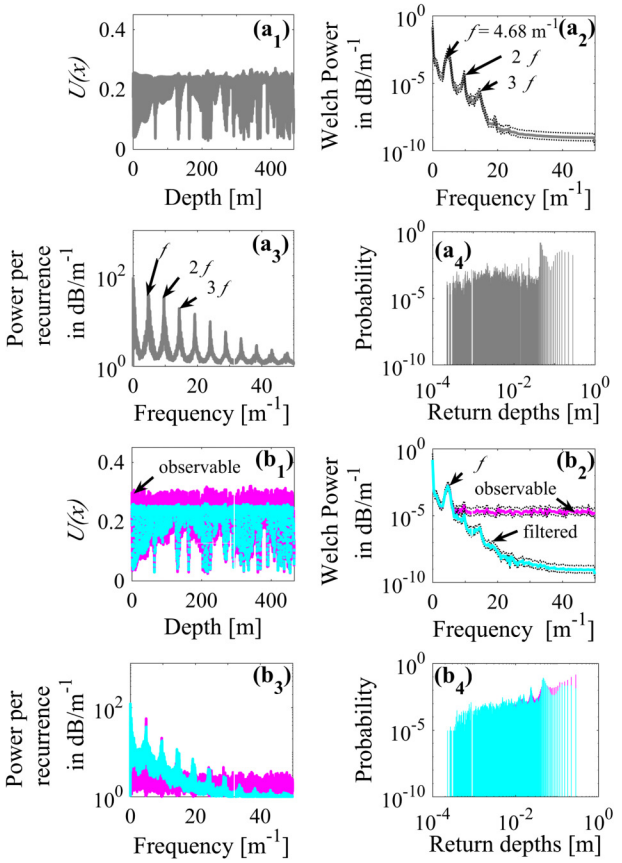

FIG. 3. Gray-Scott model (a) extracted numerical data (cf. Fig. 2) and (b) observable and nonlinearly filtered observable; the first column (1) shows the time series, the second (2) the Welch's power spectral density estimate (including 99% confidence intervals), the third column (3) gives the power spectral density based on the recurrence rate and the fourth column (4) provides the recurrence depth probabilities.

The recurrence plots of the Gray-Scott model for the noise-free as well as the noise-contaminated time series (observable) show short disrupted diagonal line segments (supplementary material, Fig. S4) indicating that the underlying processes are deterministic but not periodic and could indicate chaotic or non-stationary dynamics.[54] Using five times the standard deviation of the noise as recommended by Thiel *et al.*[63] did not change the qualitative results of the analysis for the present system.

Figure 3(a) depicts the time series, the Welch's power spectrum estimate, the recurrence power spectrum, and the recurrence time probabilities for the GSM without noise and in (b) the observable, both before and after filtering. Welch's spectrum and the recurrence spectrum show peaks after about 4.68 cycles per sample. The recurrence time probabilities for these are 14.89% for the noise-free time series and 3.39% in the case of the observable; clearly, the return depth does not show clear stable periodicities as indicated by the broad spectrum of many different probabilities encountered similar to the chaotic case of the time-continuous Rössler attractor.[8] The recurrence power spectrum is able to extract more features than Welch's power spectrum also for multiplicative noise further complementing previous findings of Zbilut *et al.*[40] or Oberst *et al.*[8] Using the nonlinear projective noise filtering algorithm *ghkss*[56] provides satisfying results which

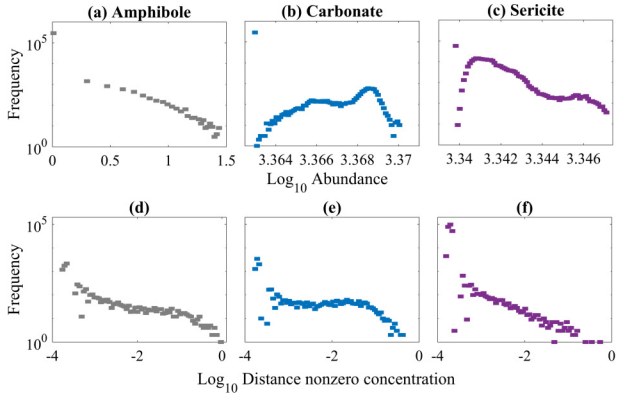

FIG. 4. Histograms (a)–(c) $\log_{10}$-concentrations and (d)–(f) log10-depth between nonzero concentrations, only bin centres are shown.

approximate the noise free data [cyan, Fig. 3(b)]; cf. Refs. 8, 61, and 47. It is studied next whether this capability of the recurrence plot-based measures to extract unstable periodic orbits in the presence of additive or multiplicative noise is going to help to distinguish between high and low dimensional, dominant dynamic processes of mineralisation.

B. Analysis of experimental core data

Figure 4 provides the statistical distribution of the logarithmic abundance (original data, upper row) and their absolutely normalised log-distances between non-zero occurrences (lower row of subfigures). The choice of taking only the nonzero events and measuring their distance homogenises the shape of the mineral distributions.

The recurrence plots and magnified areas of a data series segment of 3000 samples of amphibole, carbonate, and sericite are depicted in Fig. 5. Since we are considering map like dynamics, $\tau = 1$ represents a suitable delay. We estimated embedding dimensions of $m = 11$ for amphibole, $m = 12$ for carbonate, and $m = 10$ for sericite. For the filtering, we assumed the existence of a low dimensional manifold of dimension $q = 3$, and we applied $i = 3$ iterations.[56] As shown in Fig. 5, all recurrence plots show recurrent structures as indicated by diagonal line segments. Especially for sericite, the dynamic regimes and unstable periodic orbits are depicted as blocks, similar to those observed by Bradley and Mantilla.[37] Also, the line segments are longer and not interrupted; calculating the mean diagonal line lengths for sericite provided a mean length of 13.46 while the data of amphibole and carbonate revealed mean lengths of 6.15 and 6.04, respectively.

Figure 6 depicts the results of the recurrence power spectrum analysis, including nonlinearly filtered measurements. For amphibole and carbonate, no peaks for periodicities show up. For sericite, a period-2 cycle is detected, similar to the recurrence power spectrum of the Hénon map [supplementary material, Fig. S1(a_3)]—also compare[64] for the logistic map; its Poincaré section would show a two recurring piercing

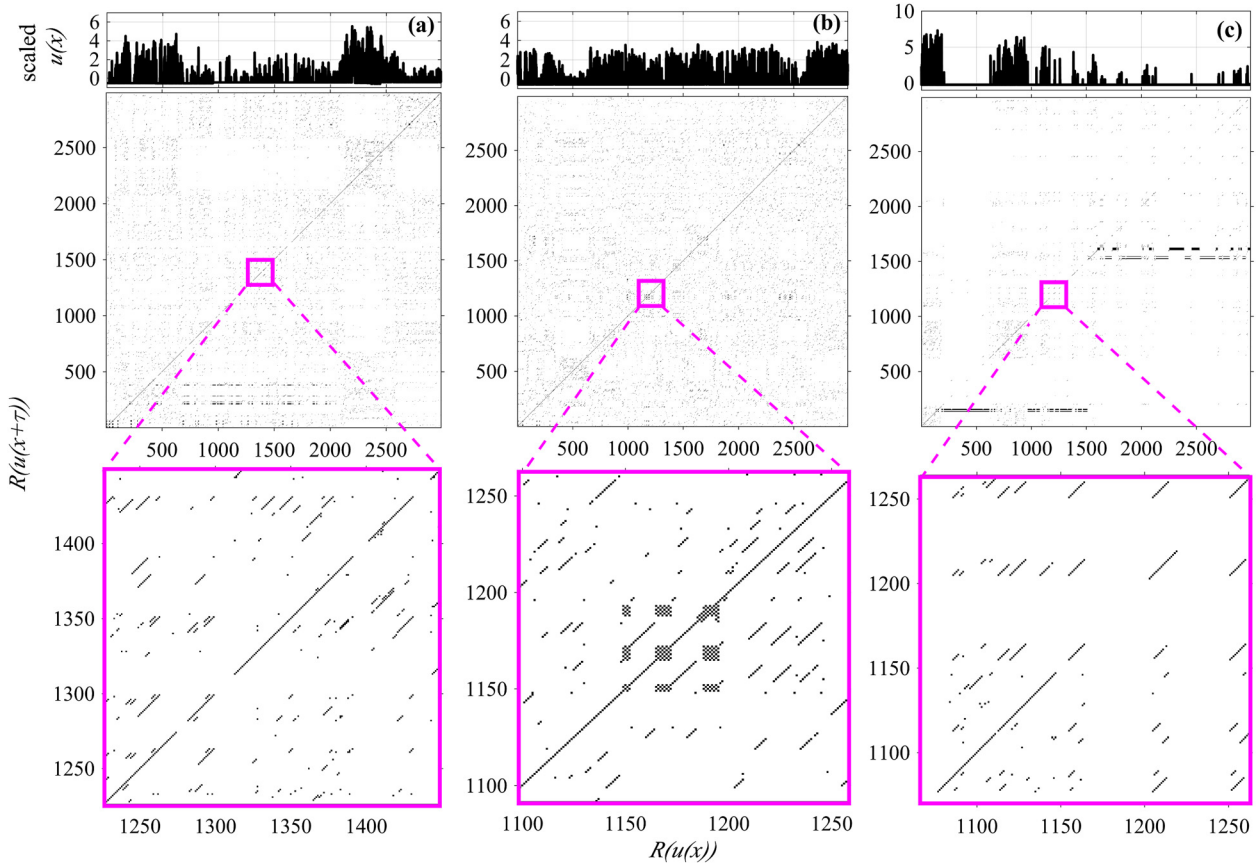

FIG. 5. Recurrence plots of the mineral data of amphibole, carbonate, and sericite using 1.5% of the normalised phase space diameter (0.056, 0.071, 0.035); magnified areas (squared) in bottom panel.

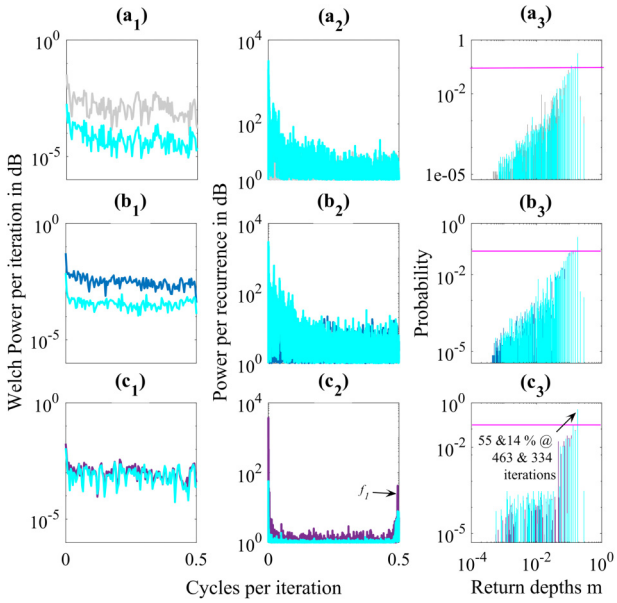

FIG. 6. Results of the recurrence spectrum analysis for (a) amphibole, (b) carbonate, and (c) sericite; left column: Welch's power spectrum estimate; middle column: recurrence power spectrum, and right column: recurrence time probability.

point.[8,9] Filtering only showed in the case of sericite some visible effect—the spectra of amphibole and carbonate remained rather broadband. Similar to the GSM, Welch's power spectrum estimates provide little information on dominant periodicities. The recurrence time probability plots are similar for amphibole and carbonate, and only accounts for sericite show higher probabilities of 14% at about 334 iterations (or 18.18 cm) and 55% at 463 iterations (or 28.57 cm) which mark two equilibrium points the system is oscillating about (Fig. 6).

Next, using unfiltered data, the average recurrence spectra based on normalised data are mapped against depth and indicate for sericite recurring periods using a window of 500 samples (supplementary material, Fig. S8). Mapping the occurrence of peaks and their locations back to their depth (Fig. 7) and using a peak picking algorithm reveals bifurcations as depicted in Fig. 8. With increasing depth a period doubling route shows up indicating period-2 (0 to 74.45 m),

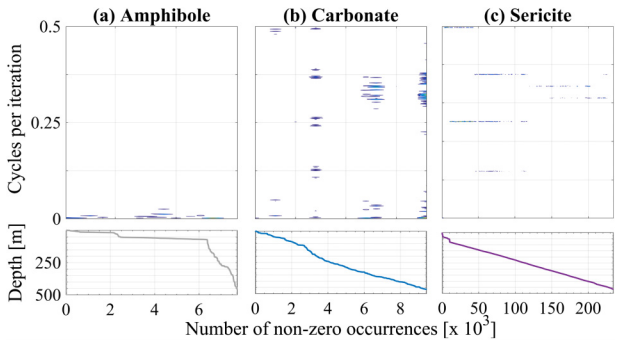

FIG. 7. Contour plots of recurrence spectra against the number of non-zero occurrences (upper panel) and mapped back against depth (lower panel) for (a) amphibole, (b) carbonate, and (c) sericite.

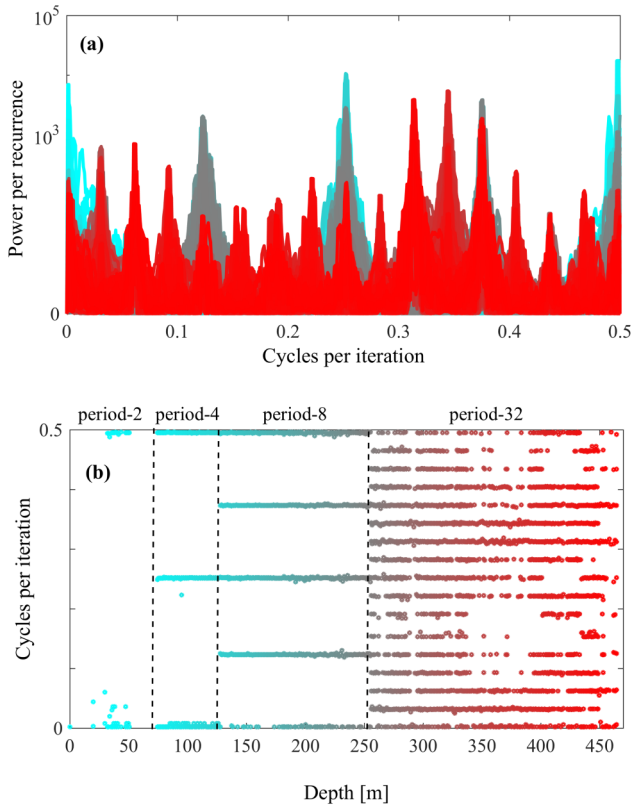

FIG. 8. Bifurcation diagram of sericite calculated by picking the peaks in the recurrence spectrum; unfiltered.

period-4 (74.45 m to 127.8 m), period-8 (127.8 m to 257.8 m), and period-32 oscillations (257.8 m to 466 m). Inverting the data series and repeating the recurrence spectra calculations provided an inverted picture of the bifurcation route to instability highlighting the causality to the measurements; using a

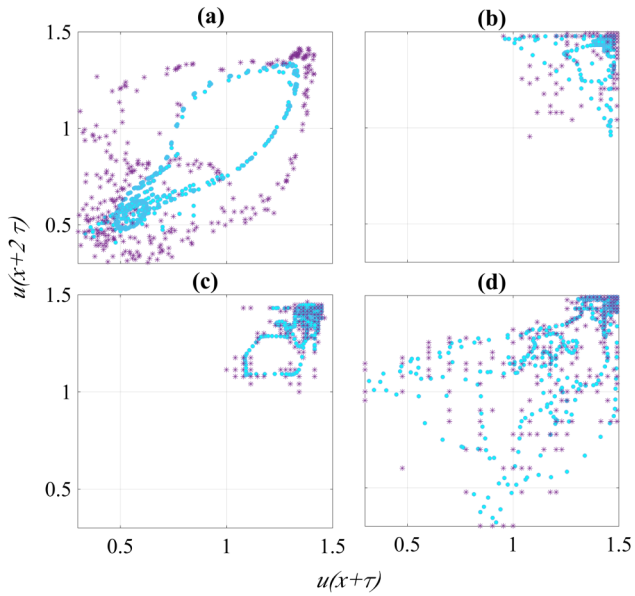

FIG. 9. Phase space plots taking the mineralisation abundance (time-continuous system) of the (a) period-2, (b) period-4, (c) period-8, and (d) period-32 behaviour; star markers (purple) indicate the measured data, and circles (bright blue) represent nonlinearly filtered data.

different sized window (1000 and 2000 samples) also did not change this behaviour.

Knowing of these dynamics, it is possible to go backwards to the original data of measured abundance to see whether it is possible to reconstruct its phase space. Figure 9 gives examples of original and filtered data for period-2, period-4, period-8, and period-32 dynamics (delay $\tau = 23$, embedding dimension $m = 7$, manifold dimension $q = 3$, and iterations $i = 8$) . By mere comparison of the original data, it is impossible to see the attracting sets, only the application of the *ghkss* filtering slightly clears up the trajectories of period-2 and period-4 regimes. However, owing to the relatively coarse amplitude resolution of the data (only integer values recorded) and the non-stationary dynamics of the system, the period-8 and period-32 orbits remain concealed.

V. DISCUSSIONS

The complexity of gold formation processes is not yet fully understood, which makes it inherently difficult to locate in a precise manner large and economically significant gold deposits without drilling test bore holes.[1,15] The chemical causes of gold precipitation, which are facilitated by temperature-pressure gradients, vary geographically[48] and arise from the interplay between numerous physico-chemical mechanisms such as fluid-rock reaction boiling and fluid mixing,[65–67] as well as chemisorption that is on surfaces of (arseno-) pyrite.[68] Considering the complexity of mineralisation processes, especially the coupled nonlinear and spatiotemporal nature of, for example, gold precipitation processes, it is astonishing that mineralising systems are yet commonly considered as being linear, having closed boundaries and with only single equilibria.[5]

We hypothesised that hydrothermal mineralising systems behave as nonlinear and deterministic dynamical systems, which can be characterised as open flow chemical reactors, oscillating far from equilibrium.[5,69] We analysed experimental mineral data of amphibole, chlorite, and sericite abundance using in geology rarely considered quantification measures, namely, the power spectrum calculated over recurrences, which is based on recurrence plots. We benchmarked our results using the Hénon map (supplementary material) as time-discrete, stationary system and the Gray-Scott reaction-diffusion equation as a non-stationary chemical system contaminated. Since all real data are contaminated by higher dimensional processes, which are either physical in nature or due to the measurement process, we also considered nonlinear filtering which is tested with additive and multiplicative noises.

Using power spectra based on recurrence plots, we successfully isolated the stable and unstable periodic oscillations in the Hénon map as well as the unstable periodic orbits of episodic fluctuations found with the Gray-Scott model. The recurrence-based measures showed for the noisy cases much better resolution than Welch's method of power spectra estimation. However, the recurrence time probability plots did not provide much information and looked broadband similar to the chaotic cases provided in Ref. 8.

The nonlinear filtering successfully removed additive and multiplicative noises. However, even though it helped clearing up the spectra, it seems to be less suitable for maps compared to the noise contaminated Gray-Scott model or the classical nonlinear Rössler system contaminated with additive noise.[8] The sparseness of the data in combination with noise could have been acting prohibitive on the filtering algorithm's ability to map the dynamics onto the manifold. Further, using multiplicative noise rendered the extraction of the true dynamics very difficult, due to the filter's high sensitivity to inaccurately estimated embedding parameters, which could be critical in cases real-life data are required to be cleaned.

By applying RP techniques to spatial data of geological drill-holes—for the first time—we identified recurring structures in geological data sets, a strong indication of (unstable) periodic orbits and a unique sign of determinism in non-equilibrium states.[39] The contour plots of recurrence spectra showed in case of amphibole recurrences only at a very low frequency while for carbonate mostly a broadband spectrum is obtained. For amphibole and carbonate, the data were very sparse, the extracted non-zero data were only about 3.25% and 3.75% of the length of the sericite data vector. Fine grained ore-bearing veins (such as gold) are generally accompanied by a strong alteration in felsic tuff wall-rocks which is characterised by quartz, sericite, calcite, and chlorite, within a pyrite/arsenopyrite matrix.[49,62] Sericite, however, indicated periodic oscillations. Picking the peaks confirms the emergence of the period doubling route to instability with increasing depth. Periodicities did not become as clearly visible in the recurrence plots nor did they show up by analysing the original mineral abundance and its phase space; as reason we assume that the data are either non-stationary or chaotic with identified periodicities referring to unstable periodic orbits. Knowing of these regimes allowed isolating and filtering of unstable periodic orbits of the original time-continuous data.

The burst-like recurrence spectra in carbonate, with no obvious structures could be a sign of deterministic chaos.[9,47] However, the rather low sampling rate of 1.6 mm resolution was prohibitive in identifying longer time series segments required for a proper attractor reconstruction and the detection of fractality.[9,51] Also, the coupling of many dimensional processes on various scales (multi-fractality, Ord *et al.*[5]) would counteract a clear separation between low and high dimensional deterministic processes, as does the spectral decomposition which, however, therefore also does not take into account nonlinear interactions between different mineral compositions. In this context, it could be interesting to link the underlying behaviour found in the recurrence spectra which we related to unstable periodic orbits to reaction phenomena observed in the GSM or other simple diffusion systems, also including a structure with porosity. The porosity model and the dynamics detected within analysed using recurrence plots could be directly linked to recurrence networks to study explicitly spatial interactions of chemical reaction diffusion reactions on different time scales.[57] Taking data from a highly sampled drill core with precipitated gold and conducting simultaneously a chemical analysis would allow a nonlinear correlation and coherence study between minerals and

chemical processes. The experimental data would then allow repeating the generation of a recurrence network for comparison with chemical processes studied in case of the GSM recurrence network to better understand gold precipitation processes.

SUPPLEMENTARY MATERIAL

Supplementary material can be found online, including details of the Hénon map, the GSM, and the time series data.

ACKNOWLEDGMENTS

AngloGold Ashanti and Silver Lake Resources are acknowledged for access to data. This project was funded by the Australian Research Council Discovery Project (Grant No. DP140104402) and supported by the German Research Council Project (Grant Nos. DFG Ho 3852/11 and DFG Ho 3852/12). The authors declare to have no competing interests.

[1]A. Bialowas, "The exploration challenge (June 2017)," *Tech. Rep.* (Minerals Council of Australia, 2017).
[2]G. Calvo, G. Mudd, A. Valero, and A. Valero, "Decreasing ore grades in global metallic mining: A theoretical issue or a global reality?," Resources **5**, 36 (2016).
[3]A. Ord, S. Oberst, R. Niven, and B. Hobbs, "What do we do with all this data? Ore exploration using modern technology," in *Gold17@Rotorua, Rotorua, New Zealand, 21–23 February 2017* (Australian Institute of Geoscientists, 2017).
[4]B. Hobbs, A. Ord, and K. Regenauer-Lieb, "The thermodynamics of deformed metmorphic rocks: A review," J. Struct. Geol. **33**, 758–818 (2011).
[5]A. Ord, B. Hobbs, and D. Lester, "The mechanics of hydrothermal systems: I. Ore systems as chemical reactors," Ore Geol. Rev. **49**, 1–44 (2012).
[6]B. Hobbs, S. Oberst, R. Niven, and A. Ord, "Mineralising systems as nonlinear dynamical systems," in *Gold17@Rotorua, Rotorua, New Zealand, 21–23 February 2017*, edited by D. Brett, T. Christie, L. Gonzales, W. Spilsbury, and J. Vearncombe (Australian Institute of Geoscientists, 2017).
[7]M. Cross and H. Greenside, *Pattern Formation and Dynamics in Nonequilibrium Systems* (Cambridge University Press, 2009).
[8]S. Oberst, S. Marburg, and N. Hoffmann, "Determining periodic orbits via nonlinear filtering and recurrence spectra in the presence of noise," Procedia Eng. **199**, 772–777 (2017).
[9]H. G. Schuster and W. Just, *Deterministic Chaos* (Wiley-VCH, 2005).
[10]P. Gaspard, "Nonequilibrium nanosystems," in *Nonlinear Dynamics of Nanosystems*, edited by G. Radons, B. Rumpf, and H. G. Schuster (Wiley-VCH, Weinheim, 2010).
[11]L. Arnold, *Random Dynamical Systems* (Springer-Verlag, Berlin, 1998).
[12]V. Anishchenko, V. Astakhov, A. Neiman, T. Vadivasova, and L. Schimansky-Geier, *Nonlinear Dynamics of Chaotic and Stochastic Systems* (Springer-Verlag, Berlin, 2007).
[13]D. Lester, A. Ord, and B. Hobbs, "The mechanics of hydrothermal systems: II. Fluid mixing and chemical reactions," Ore Geol. Rev. **49**, 45–71 (2012).
[14]A. Ord, M. Munro, and B. Hobbs, "Hydrothermal mineralising systems as chemical reactors: Wavelet analysis, multifractals and correlations," Ore Geol. Rev. **79**, 155–179 (2016).
[15]S. Oberst, R. Niven, A. Ord, B. Hobbs, and D. Lester, "Application of recurrence plots to orebody exploration data," in *Target 2017, Innovating now for our future, Uniclub, University of Western Australia, Perth, Australia, 19–21 April* (2017).
[16]D. Lynch, T. Rogers, and S. Wanke, "Chaos in a continuous stirred tank reactor," Math. Model. **3**, 103–116 (1982).
[17]J. Vastano, J. Pearson, W. Horsthemke, and H. Swinney, "Chemical pattern formation with equal diffusion coefficients," Phys. Lett. A **124**, 320–324 (1987).
[18]M. Stich, G. Ghoshal, and J. Paurez-Mercader, "Parametric pattern selection in a reaction-diffusion model," PLoS One **8**, 1–6 (2013).
[19]J. McGough and K. Riley, "Pattern formation in the gray-scott model," Nonlinear Anal. Real World Appl. **5**, 105–121 (2004).
[20]P. Gray and S. Scott, *Chemical Oscillations and Instabilities* (Oxford University Press, Oxford, 1990).
[21]R. Henley and B. Berger, "Self-ordering and complexity in epizonal mineral deposits," Ann. Rev. Earth Planet. Sci. **28**, 669–719 (2000).
[22]*Nonlinearity and Chaos in Engineering Dynamics*, 2nd ed., edited by J. Thompson and S. Bishop (John Wiley & Sons Ltd., New York, 2002).
[23]G. Kerschen, K. Worden, A. F. Vakakis, and J. C. Golinval, "Past, present and future of nonlinear system identification in structural mechanics," Mech. Syst. Signal Process. **20**, 505–592 (2006).
[24]K. Worden, C. R. Farrar, J. Haywood, and M. Todd, "A review of nonlinear dynamics applications to structural health monitoring," Struct. Control Health Monit. **15**, 540–567 (2008).
[25]S. Oberst and J. Lai, "Nonlinear transient and chaotic interactions in disc brake squeal," J. Sound Vib. **342**, 272–289 (2015).
[26]M. Riedl, N. Marwan, and J. Kurths, "Multiscale recurrence analysis of spatio-temporal data," Chaos **25**, 123111 (2015).
[27]Physical assemblages of alteration minerals due to metasomatism. Metasomatism substitutes chemically the original rock mineral phases with new phases, which is facilitated by fluid flux associated with chemical reactants aqueous product removal.[70]
[28]J.-P. Eckmann, S. Oliffson Kamphorst, and D. Ruelle, "Recurrence plots of dynamical systems," Europhys. Lett. **4**, 973–977 (1987).
[29]J. Zaldivar, F. Strozzi, S. Dueri, D. Marinov, and J. Zbilut, "Characterization of regime shifts in environmental time series with recurrence quantification analysis," Ecol. Modell. **210**, 58–70 (2008).
[30]G.-F. Fan, L.-L. Peng, W.-C. Hong, and F. Sun, "Kinetics for reduction of iron ore based on the phase space reconstruction," J. Appl. Math. **514851**, 1–10 (2014).
[31]D. Eroglu, N. Marwan, S. Prasad, and J. Kurths, "Finding recurrence networks' threshold adaptively for a specific time series," Nonlinear Process. Geophys. **21**, 1085–1092 (2014).
[32]G. Filligoi and F. Felici, "Detection of hidden rhythms in surface {EMG} signals with a non-linear time-series tool," Med. Eng. Phys. **21**, 439–448 (1999).
[33]K. Guhathakurta, B. Bhattacharya, and A. Chowdhurya, "Using recurrence plot analysis to distinguish between endogenous and exogenous stock market crashes," Physica A **389**, 1874–1882 (2010).
[34]S. Oberst and J. Lai, "Chaos in brake squeal noise," J. Sound Vib. **330**, 955–975 (2011).
[35]B. A. Wernitz and N. P. Hoffmann, "Recurrence analysis and phase space reconstruction of irregular vibration in friction brakes: Signatures of chaos in steady sliding," J. Sound Vib. **331**, 3887–3896 (2012).
[36]C. Goldfinger, C. Nelson, and J. Johnson, "Holocene earthquake records from the Cascadia subduction zone and northern San Andreas fault based on precise dating of offshore turbidites," Ann. Rev. Earth Planet. Sci. **31**, 555–577 (2003).
[37]E. Bradley and R. Mantilla, "Recurrence plots and unstable periodic orbits," Chaos **12**, 596–600 (2003).
[38]I. Berenstein and J. Carballido-Landeira, "Spatiotemporal chaos involving wave instability," Chaos **27**, 013116 (2017).
[39]R. Gilmore and M. Lefranc, *Topology Analysis of Chaos* (Wiley VCH Verlagsgesellschaft, 2002).
[40]J. Zbilut and N. Marwan, "The Wiener-Khinchin theorem and recurrence quantification," Phys. Lett. A **372**, 6622–6626 (2007).
[41]P. Maini, K. Painter, and H. . Chau, "Spatial pattern formation in chemical and biological systems," J. Chem. Soc. Faraday Trans. **93**, 3601–3610 (1997).
[42]C. Mocenni, A. Facchini, and A. Vicino, "Identifying the dynamics of complex spatio-temporal systems by spatial recurrence properties," Proc. Nat. Acad. Sci. USA **107**, 8097–8102 (2010).
[43]A. Turing, "The chemical basis of morphogenesis," Philos. Trans. R. Soc. Lond. B Biol. Sci. **237**, 37–72 (1952).
[44]D. I. Groves, "The crustal continuum model for late-Archaean lode-gold deposits of the Yilgarn Block, Western Australia," Miner. Depos. **28**, 366–374 (1993).
[45]D. Morgan, A. Doelman, and T. Kaper, "Stationary periodic pattern in the 1d Gray-Scott model," Methods Appl. Anal. **7**, 105–150 (2000).
[46]A. Spanos, *Probability Theory and Statistical Inference* (Cambridge University Press, UK, 1999).
[47]S. Oberst and J. Lai, "A statistical approach to estimate the Lyapunov spectrum in disc brake squeal," J. Sound Vib. **334**, 120–135 (2015).
[48]A. Tomkins, "On the source of orogenic gold," Geology **41**, 1255–1256 (2013).

[49]Y. Zhu, F. An, and J. Tan, "Geochemistry of hydrothermal gold deposits: A review," Geosci. Front. **2**, 367–374 (2011).
[50]V. Winschel and M. Krätzig, "Solving, estimating, and selecting nonlinear dynamic models without the curse of dimensionality," Econometrica **78**, 803–821 (2010).
[51]H. Kantz and T. Schreiber, *Nonlinear Time Series Analysis* (Cambridge University Press, 2004).
[52]F. Takens, "Detecting strange attractors in turbulence," in *Dynamical Systems and Turbulence*, Lecture Notes in Mathematics Vol. 898 (Springer Nature, Switzerland, 1981), pp. 366–381.
[53]H. D. I. Abarbanel, *Analysis of Observed Chaotic Data* (Springer, New York, 1996).
[54]N. Marwan, M. Carmen Romano, M. Thiel, and J. Kurths, "Recurrence plots for the analysis of complex systems," Phys. Rep. **438**, 237–329 (2007).
[55]A. M. Fraser and H. L. Swinney, "Independent coordinates for strange attractors from mutual information," Phys. Rev. A **33**, 1134–1140 (1986).
[56]R. Hegger and H. Kantz, "Practical implementation of nonlinear time series methods: The TISEAN package," Chaos **9**, 413–435 (1999).
[57]R. Donner, Y. Zou, N. Donges, J. F. Marwan, and J. Kurths, "Recurrence networks-a novel paradigm for nonlinear time series analysis," New J. Phys. **12**, 033025 (2010).
[58]N. Marwan and J. Kurths, "Nonlinear analysis of bivariate data with cross-recurrence plots," Phys. Lett. A **302**, 299–307 (2002).
[59]E. Ngamga, D. Senthilkumar, A. Prasad, P. Parmananda, J. Marwan, and N. Kurths, "Distinguishing dynamics using recurrence-time statistics," Phys. Rev. E **85**, 026217 (2012).
[60]R. Randall, *Frequency Analysis* (Bruel & Kjaer, Copenhagen, 1987).
[61]S. Oberst, J. C. S. Lai, and T. A. Evans, "An innovative signal processing technique for the extraction of ants' walking signals," Acoust. Aust. **43**(1), 87–96 (2015).
[62]G. Phillips and R. Powell, "Formation of gold deposits: Review and evaluation of the continuum model," Earth Sci. Rev. **94**, 1–21 (2009).
[63]M. Thiel, M. C. Romano, J. Kurths, R. Meucci, E. Allaria, and F. T. Arecchi, "Influence of observational noise on the recurrence quantification analysis," Physica D **171**, 138–152 (2002).
[64]X. Wang and Q. Liang, "Reverse bifurcation and fractal of the compound logistic map," Commun. Nonlinear Sci. Numer. Simul. **13**, 913–927 (2008).
[65]D. Weatherley and R. Henley, "Flash vaporization during earthquakes evidenced by gold deposits," Nat. Geosci. **6**, 294–298 (2013).
[66]K. Evans, G. Phillips, and R. Powell, "Rock-buffering of auriferous fluids in altered rocks associated with the Golden Milestyle mineralization, Kalgoorlie gold field, Western Australia," Econ. Geol. **101**, 805–817 (2006).
[67]R. Bateman and S. Hagemann, "Gold mineralisation throughout about 45 ma of archaean orogenesis: Protracted flux of gold in the golden mile, Yilgarn craton, western australia," Miner. Depos. **39**, 536–559 (2004).
[68]P. Möller and G. Kersten, "Electrochemical accumulation of visible gold on pyrite and arsenopyrite surfaces," Miner. Depos. **29**, 404–413 (1994).
[69]B. E. Hobbs and A. Ord, *The Mechanics of Deforming Metamorphic Rocks* (Elsevier, 2015).
[70]R. W. Luth, "The mantle and core," in *Treatise on Geochemistry* (Elsevier-Pergamon, Oxford, 2003), Vol. 2, pp. 319–361.